Synthesis of Nanosized $(1-x)NaNbO_3-xSrTiO_3$ Solid Solution by Mechanochemical Activation, Processing of Ceramics, and Phase Transitions

T. Hungría,[†,‡] M. Algueró,[†] and A. Castro*[,†]

Instituto de Ciencia de Materiales de Madrid (ICMM), CSIC, Cantoblanco, 28049 Madrid, Spain, and Centre d'Elaboration de Matériaux et d'Etudes Structurales (CEMES), CNRS, 29, rue Jeanne Marvig, BP 94347, 31055 Toulouse, France

Received June 23, 2006. Revised Manuscript Received August 30, 2006

A novel mixed technique based on wet-chemistry plus mechanochemical activation has been applied to obtain the $Na_{1-x}Sr_xNb_{1-x}Ti_xO_3$ solid solution with $x = 0.1$, 0.25, 0.5, 0.75, and 0.9. The wet-chemistry step aims at a better mixing of the constituent elements before the mechanical treatment, and thus, at a better reactivity during the activation step. Milled powders were studied by thermogravimetry (TG), differential thermal analysis (DTA), and X-ray diffraction (XRD). Incipient formation of a perovskite-type oxide of the $NaNbO_3-SrTiO_3$ system by mechanosynthesis at room temperature was observed in the whole range of compositions. Mechanical treatment was followed by annealing at different temperatures to establish the optimized protocol for the synthesis of each member of the solid solution, as a single phase, with very important decreases in the formation temperatures (up to 600 °C) and reaction times (several days), as compared with the traditional ceramic method due to the high reactivity of the mechanically activated powders. Dense ceramics can be processed from these mechanosynthesized precursors. The ceramic samples were used to study phase transitions in the solid solution by measurement of the dielectric permittivity as a function of the temperature.

Introduction

Piezoelectric materials based on lead compounds are widely used due to their exceptional piezoelectric, pyroelectric, and ferroelectric properties. However, lead has been recently retired from many commercial applications owing to concerns regarding its toxicity and possible ecological hazard. Alkaline niobates-based piezoceramics possess a unique combination of electrical and mechanical properties: low mass density, high sound velocity, a wide range of dielectric permittivities and mechanical Q's, and fairly high electromechanical coupling factors and piezoelectric coefficients.[1] For these reasons, in recent years, some alkaline niobate-based ceramics have attracted much attention as an environmental friendly alternative for the substitution of commercial piezoceramics based on lead.[2]

Sodium niobate, $NaNbO_3$, is antiferroelectric at room temperature,[3] but the application of an electric field or the substitution of Li[4] or K[5] for Na induce a ferroelectric phase that provides piezoelectric activity, which is interesting for high-frequency devices.[6] It is known that $NaNbO_3$ presents a large number of structural phases, variants of lower symmetry of the ideal perovskite structure, having six phase transitions from the nonpolar high-temperature phase to the antiferroelectric room-temperature phase and the low-temperature ferroelectric one.[7] Recent studies are focused on the analysis, involving structural characterization and dielectric measurements, of the phase transitions of $NaNbO_3-ABO_3$ systems.[1,8,9] In the case of $NaNbO_3-SrTiO_3$, although both $NaNbO_3$ and $SrTiO_3$ have been extensively studied, the solid solution between the two oxides has received less attention. Dielectric measurements of $Na_{1-x}Sr_xNb_{1-x}Ti_xO_3$ revealed an antiferroelectric to ferroelectric transition at $x = 0.2$[10] and piezoelectric studies show that the coefficient K_p rises monotonically with increasing $SrTiO_3$ content.[1]

More recently, Xu et al.[11] studied the $Na_{1-x}Sr_xNb_{1-x}Ti_xO_3$ solid solution from the viewpoint of the synthesis by sol−gel and solid-state synthesis and crystal chemistry. Moreover, a detailed investigation on the enthalpies of formation and of morphotrophic transitions was also carried out. However, a description of the processing of ceramics and of their

* To whom correspondence should be addressed. Tel.: (+34) 91 334 9000. Fax: (+34) 91 372 0623. E-mail: acastro@icmm.csic.es.
† ICMM, CSIC.
‡ CEMES, CNRS.

(1) Reznichenko, L. A.; Dergunova, N. V.; Geguzina, G. A.; Razumovskaya, O. N.; Shilkina, L. A.; Ivanova, L. S. *Inorg. Mater.* **1997**, *33*, 1277.
(2) Saito, Y.; Takao, H.; Tani, T.; Nonoyama, T.; Takatori, K.; Homma, T.; Nagaya, T.; Nakamura M. *Nature* **2004**, *432*, 84.
(3) Cross, L. E.; Nicholson, B. J. *Philos. Mag.* **1955**, *46*, 453.
(4) Nitta, T. *J. Am. Ceram. Soc.* **1968**, *51*, 626.
(5) Shirane, G.; Newnham, R.; Pepinsky, R. *Phys. Rev.* **1954**, *96*, 581.
(6) Jimenez, B.; Castro, A.; Pardo, L. *Appl. Phys. Lett.* **2003**, *82*, 3940.
(7) Megaw, H. D. *Ferroelectrics* **1974**, *7*, 87.
(8) Raevski, I. P.; Reznitchenko, L. A.; Malitskaya, M. A.; Shilkina, L. A.; Lisitsina, S. O.; Raevskaya, S. I.; Kuznetsova, E. M. *Ferroelectrics* **2004**, *299*, 95.
(9) Bahri, F.; Khemakhem, H.; Gargouri, M.; Simon A.; Von der Muhll, R.; Ravez, J. *Solid State Sci.* **2003**, *5*, 1445.
(10) Glaister, R. M. *J. Am. Ceram. Soc.* **1960**, *43*, 348.
(11) Xu, H. W.; Navrotsky, A.; Su, Y. L.; Balmer, M. L. *Chem. Mater.* **2005**, *17*, 1880.

10.1021/cm0614618 CCC: $33.50
Published on Web 09/28/2006

dielectric properties as a function of temperature, which provides information of the phase transitions, is missed in the literature. $SrTiO_3$ represents the prototype of the ideal perovskite structure (cubic, space group $Pm\bar{3}m$) constituted by a three-dimensional framework of corner-sharing TiO_6 octahedra, with Sr cations occupying the cuboctahedrical cavities. The room-temperature structure of $NaNbO_3$ is also based on the perovskite structure, but in this case, the framework is built up from tilted NbO_6 octahedra and for this reason it is orthorhombic. As was mentioned above, on heating, $NaNbO_3$ undergoes transitions to phases with higher symmetry and becomes cubic. This transition sequence is complex and may depend on the thermal history of the samples.[12] Xu et al. described a similar sequence of transitions with increasing Sr−Ti content in the series $NaNbO_3$−$SrTiO_3$, and thus, the $Na^+ + Nb^{5+} \rightarrow Sr^{2+} + Ti^{4+}$ substitution mimics temperature effects on the $NaNbO_3$ distorted perovskite.

Due to the good results obtained in the synthesis of other three-dimensional and layered perovskites,[13−16] mechanochemical activation routes have been used to prepare the $(1-x)NaNbO_3-xSrTiO_3$ solid solution. Oxides with perovskite-type structure are usually prepared by the conventional ceramic method, but high temperature and long reaction times are required, which yield powders that are not suitable for the preparation of high-performance ceramics. This is so because very inhomogeneous particle size distributions are obtained and a certain level of impurity content is difficult to avoid. Mechanical treatment is a very efficient way to modify the conditions in which chemical reactions usually take place because high-energy milling produces disorder in the crystal and generation of defects that cause the decrease of the activation barrier.[17] During the high-energy milling, the particle size of the crystals is reduced, the homogeneity of the mixture is increased, and in most of cases the solid becomes more reactive.[18] Furthermore, the high reactivity and low particle size obtained facilitate the sintering process, making it thus possible to obtain high-density ceramics at low temperatures.[19] Particularly, for alkaline niobate ceramics, control of the processing conditions is required to improve the compositional homogeneity since high temperature and long reaction times produce the volatilization of the alkaline metal.

This paper describes a study of routes based on high-energy milling to improve the reaction conditions to synthesize the $Na_{1-x}Sr_xNb_{1-x}Ti_xO_3$ solid solution and to allow the processing of dense ceramics at lower temperature. The dielectric properties of the ceramics processed from nanosized powders are also characterized as a function of temperature and frequency as a means to study phase transitions in the system.

Experimental Procedures

Two different procedures have been used to synthesize the $Na_{1-x}Sr_xNb_{1-x}Ti_xO_3$ ($x = 0.1$, 0.25, 0.5, 0.75, and 0.9) samples: conventional solid-state reaction and a mixed technique of wet chemistry plus mechanochemical activation. For the conventional ceramic route, stoichiometric mixtures of analytical-grade Na_2CO_3, $SrCO_3$, Nb_2O_5, and TiO_2 were initially homogenized by hand in an agate mortar and thermally treated at increasing temperatures from 500 to 1250 °C, each temperature maintained for different lengths of time, with intermediate regrinding and X-ray characterization.

In the case of the mixed technique, the wet chemistry step aims at a better mixing of the constituent elements before the mechanical treatment and, thus, a better reactivity during the activation step.[20] For each composition, NaOH was dissolved in deionized water and stoichiometric quantities of insoluble reactants ($Sr(OH)_2 \cdot 8H_2O$, TiO_2, and Nb_2O_5) were added into the aqueous solution. The suspensions were stirred for 4 h and then dried at 150 °C overnight to obtain the precursor for the mechanical treatment step in a planetary mill (Fritsch Pulverisette 6). The precursors (4 g) were placed in a stainless-steel vessel with five steel balls 2 cm in diameter and 35 g in weight, the grinding bowl being rotated at 200 rpm. All mechanochemical treatments were carried out in air, for times up to 125 h.

Crystallographic evolution during mechanical activation and subsequent thermal treatment of the different mixtures was investigated by XRD with a Bruker AXS D8 Advance diffractometer. The patterns were recorded between 5° and 60° (2Θ), with 2Θ increments of 0.1° and a counting time of 1.5 s per step. The Cu Kα doublet ($\lambda = 0.15418$ nm) was used in these X-ray experiments. For more detailed X-ray studies, a Philips X'pert diffractometer fitted with a primary Ge(111) monocromator (Cu $K\alpha_1$ radiation, $\lambda = 0.15406$ nm) was used. Slow scans with a step size of 0.02° and step time of 2 s were carried out. To obtain the lattice parameter, least-square methods were applied to these data, and Silicon (NIST standard reference material 640b, $a = 0.5430940 \pm 0.0000035$ nm for $\lambda CuK\alpha_1$) was added as standard to reduce errors associated with lattice parameters calculations.

The thermal behavior of the activated mixtures was investigated by differential thermal (DTA) and thermogravimetric analysis (TG). The measurements were carried out in air, from room temperature to 1000 °C, using a Seiko 320 instrument, with α-Al_2O_3 as the inert reference material. The heating−cooling rates were 10 °C min^{-1} and the quantity of sample used was about 10 mg. The evolved gases were analyzed with a Pfeiffer ThermoStar GSD 301 T (quadrupole mass spectrometer), with argon as gas carrier to determine the molar mass.

Transmission electron microscopy (TEM) images and selected area electron diffraction (SAED) patterns were taken in a JEOL 2000-FX TEM, working at 200 kV. For these studies, samples were crushed in an agate mortar and suspended in *n*-butanol. After ultrasonic dispersion, a droplet was deposited on a copper grid supporting a perforated carbon film. To confirm grain size obtained from XRD data, the particle size distribution of the mechanosynthesized samples was obtained by Feret's[21] diameter from several TEM images of each sample.

The determination of the density of the isolated phases was carried out with an Accupyc 1330 pycnometer using the helium displacement technique.

Mechanosynthesized powders were used as precursors to process $Na_{1-x}Sr_xNb_{1-x}Ti_xO_3$ ($x = 0.1$, 0.25, 0.5, 0.75, and 0.9) ceramics.

(12) Pozdnyakova, I.; Navrotsky, A.; Shilkina, L.; Reznitchenko, L. *J. Am. Ceram. Soc.* **2002**, *85*, 379.
(13) Hungría, T.; Hungría, A. B.; Castro, A. *J. Solid State Chem.* **2004**, *177* (4-5), 1559.
(14) Hungría, T.; Lisoni, J. G.; Castro, A. *Chem. Mater.* **2002**, *14*, 1747.
(15) Hungría, T.; Algueró, M.; Hungría, A. B.; Castro, A. *Chem. Mater.* **2005**, *17*, 6205.
(16) Ferrer, P.; Iglesias, J. E.; Castro, A. *Chem. Mater.* **2004**, *16*, 1323.
(17) Boldyrev, V. V.; Tkacova, K. *J. Mater. Synth. Proc.* **2000**, *8*, 121.
(18) Vidojkovic, V. M.; Brankovic, A. R.; Milosevic, S. D. J. *Mater. Lett.* **1997**, *31*, 55.
(19) Moure, A.; Castro, A.; Pardo, L. *Acta Mater.* **2004**, *52*, 945.
(20) Hungría, T.; Pardo, L.; Moure, A.; Castro, A. *J. Alloy. Compd.* **2005**, *395*, 166.
(21) Matyi, R.; Schwartz, L.; Butt, J. *Catal. Rev.* **1987**, *29*, 41.

Table 1. Phases Identified after Different Thermal Treatments of the Stoichiometric Mixtures by the Ceramic Route[a]

mixtures $(1-x)/2Na_2CO_3$: $xSrCO_3$: $(1-x)/2Nb_2O_5$:$xTiO_2$	T (°C)/t (h or days)	phases
$x = 0.1$	700 °C/12 h	$NaNbO_3 + Na_2Nb_4O_{11} + Nb_2O_5$
	900 °C/12 h	NNST + $SrNb_{tr}$
	1200 °C/12 h	**$Na_{0.9}Sr_{0.1}Nb_{0.9}Ti_{0.1}O_3$**
$x = 0.25$	700 °C/12 h	$NaNbO_3 + SrCO_3 + Na_2Nb_4O_{11}$
	900 °C/12 h	NNST + SrNb
	1200 °C/12 h	**$Na_{0.75}Sr_{0.25}Nb_{0.75}Ti_{0.25}O_3$**
$x = 0.5$	700 °C/12 h	$NaNbO_3 + SrCO_3 + TiO_2$
	900 °C/12 h	NNST + SrNb + STn
	1200 °C/12 h	**$Na_{0.5}Sr_{0.5}Nb_{0.5}Ti_{0.5}O_3$**
$x = 0.75$	700 °C/12 h	$SrCO_3 + SrTiO_3 + Na_2CO_3 + TiO_2$
	900 °C/12 h	$SrTiO_3$ + STn + SrNb
	1200 °C/1 d	**$Na_{0.25}Sr_{0.75}Nb_{0.25}Ti_{0.75}O_3$**
$x = 0.9$	700 °C/12 h	$SrCO_3 + SrTiO_3 + TiO_2$
	900 °C/12 h	$SrTiO_3$ + STn + SrNb
	1250 °C/3 d	**$Na_{0.1}Sr_{0.9}Nb_{0.1}Ti_{0.9}O_3$**

[a] STn = mixture of $Sr_2[Sr_{n-1}Ti_nO_{3n+1}]$ phases, SrNb = mixture of oxides of Sr and Nb, NNST = perovskite of the system $Na_{1-x}Sr_xNb_{1-x}Ti_xO_3$, tr = traces.

Sintering was accomplished in air, at temperatures from 1200 to 1350 °C with a heating rate of 3 °C min^{-1}. Powders were shaped by uniaxial pressing at 21 MPa as thin disks of 10 mm diameter and 2 mm thickness. These disks were then isostatically pressed at 200 MPa, and finally conventional sintering was carried out on a Pt foil.

The density of the ceramics was obtained by the Archimedes' method with deionized water. Phases and crystal structure were studied by XRD. Microstructure was characterized on polished (up to 0.3 μm alumina) and thermally etched/quenched surfaces by optical microscopy with a Leitz Laborlux 12 ME S/ST optical apparatus.

Ag electrodes were painted on the major faces of thinned ceramic discs and sintered at 650 °C for electrical characterization. The dependence of the dielectric permittivity on temperature at 10 frequencies between 1 kHz and 1 MHz was measured with a HP4194A impedance/gain phase analyzer, during a heating/cooling cycle between room temperature and 300 °C with a 1 °C min^{-1} rate. Additional measurements were carried out from 77 to 550 K during heating at 1.5 °C min^{-1} with a HP4192A impedance analyzer between 100 Hz and 1 MHz.

Results and Discussion

Conventional Ceramic Route. Results of the experiments of solid-state synthesis from the stoichiometric mixtures of Na_2CO_3, $SrCO_3$, Nb_2O_5, and TiO_2 are summarized in Table 1. In the cases of high Na−Nb contents ($x = 0.1$, 0.25, and 0.5), $NaNbO_3$ is the major phase after thermal treatment at 700 °C. Perovskites of the $Na_{1-x}Sr_xNb_{1-x}Ti_xO_3$ system are obtained after treatment at 900 °C, but in coexistence with a mixture of strontium−niobium oxides with stoichiometries so varied as Sr_5NbO_4, $Sr_2Nb_{10}O_{27}$, $Sr_4Nb_2O_9$, and $Sr_5Nb_4O_{15}$, which remained stable up to 1200 °C. For the $x = 0.75$ and 0.9 compositions, a small quantity of $SrTiO_3$ was obtained after heating at 700 °C. In these cases, the formation of a mixture of different Ruddlesden−Popper phases was observed as secondary phases in addition to the strontium niobium oxides. In the case of $Na_{0.1}Sr_{0.9}Nb_{0.1}Ti_{0.9}O_3$, a thermal treatment of 1250 °C for 3 days was necessary to obtain the perovskite as single phase. In general, it can be said that higher Na−Nb contents resulted in lower $Na_{1-x}Sr_xNb_{1-x}Ti_xO_3$ synthesis temperatures.

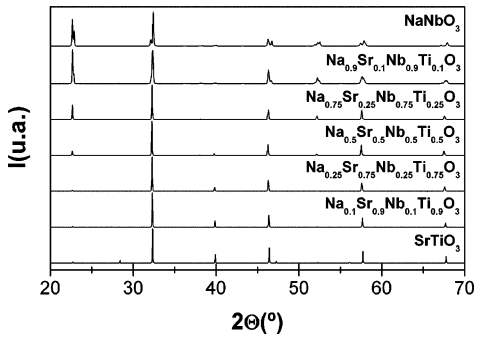

Figure 1. XRD patterns of the phases $Na_{1-x}Sr_xNb_{1-x}Ti_xO_3$ ($x = 0$, 0.1, 0.25, 0.5, 0.75, 0.9, and 1) obtained by the ceramic route from stoichiometric mixtures of Na_2CO_3, $SrCO_3$, Nb_2O_5, and TiO_2.

Figure 1 shows the X-ray diffraction patterns of the final products obtained for each composition, including the $x = 0$ and 1 for the sake of comparison. For all compositions, a perovskite-type oxide was obtained as single phase and, as was expected, higher Sr−Ti contents imply a higher symmetry structure.

Table 2 summarizes the lattice parameters for $Na_{1-x}Sr_xNb_{1-x}Ti_xO_3$ ($x = 0.1$, 0.25, 0.5, 0.75, and 0.9) phases calculated from XRD data by least-square methods, taking as starting structural models data reported from the following ICDD files: 33-1270 for $NaNbO_3$ (*Pbma*, $a = 0.5568$, $b = 1.552$, and $c = 0.5504$ nm), 86-0229 for $Na_{0.7}Sr_{0.3}Nb_{0.7}Ti_{0.3}O_3$ (*Pmmn*, $a = 0.78294$, $b = 0.78298$, and $c = 0.78482$ nm), 85-2008 for $Na_{0.3}Sr_{0.7}Nb_{0.3}Ti_{0.7}O_3$ (*I*4/*mmm*, $a = 0.78336$ and $c = 0.78482$ nm), and 35-0734 for $SrTiO_3$ ($Pm\bar{3}m$, $a = 0.3905$ nm).

With increasing Sr−Ti content, the crystallographic symmetry of the oxides becomes higher, from orthorhombic for $x = 0.1$, 0.25, and 0.5 to tetragonal in the case of $x = 0.75$ and finally cubic for $x = 0.9$. These compositionally induced transitions are analogous to those described in the $NaNbO_3$ compound on heating, such as it was pointed out by Xu et al.,[11] although the observed symmetry of the compositions with $x = 0.5$ and 0.75 are not the same in both studies. This fact is probably due to the different thermal histories of the samples.

Mechanochemical Activation Route. The precursors obtained after the wet-chemistry step for each composition were characterized by XRD and found to be formed by crystalline TiO_2 anatase, Nb_2O_5, strontium hydroxides, and a Na-rich amorphous fraction. Then, these precursors were mechanochemically activated in a planetary mill during different milling times. Figure 2 shows the XRD patterns of the precursor corresponding to the $0.9NaNbO_3-0.1SrTiO_3$ ($x = 0.1$) composition at increasing milling times. Two steps were observed during the milling process: an initial diminution of particle size in the precursor and a subsequent solid-state reaction in the activated mixture. The diffraction peaks of a perovskite of the system $Na_{1-x}Sr_xNb_{1-x}Ti_xO_3$ (in general, hereafter referred to as NNST) could be clearly observed after 20 h of milling and further activation produced an increase in the perovskite crystallinity. The sample obtained

Table 2. Unit-Cell Parameters of the Different $Na_{1-x}Sr_xNb_{1-x}Ti_xO_3$ Phases Obtained by the Traditional Ceramic Route[a]

phase	S.G.	*a* (Å)	*b* (Å)	*c* (Å)	ρ_{powder} (g cm^{-3})	ρ_{DRX} (gcm^{-3})
$Na_{0.9}Sr_{0.1}Nb_{0.9}Ti_{0.1}O_3$	*Pbma*	5.520(3)	15.542(7)	5.550(3)	4.590(4)	4.627
$Na_{0.75}Sr_{0.25}Nb_{0.75}Ti_{0.25}O_3$	*Pmmn*	7.832(1)	7.8310(9)	7.8459(9)	4.625(2)	4.659
$Na_{0.5}Sr_{0.5}Nb_{0.5}Ti_{0.5}O_3$	*Pmmn*	7.8381(9)	7.8381(9)	7.8521(7)	4.756(6)	4.783
$Na_{0.25}Sr_{0.75}Nb_{0.25}Ti_{0.75}O_3$	*I*4/*mmm*	7.8325(8)		7.830(1)	4.894(8)	4.938
$Na_{0.1}Sr_{0.9}Nb_{0.1}Ti_{0.9}O_3$	*Pm*$\bar{3}$*m*	3.9092(3)			5.017(3)	5.045

[a] S.G. = space group, ρ_{powder} = experimental density of the powder, ρ_{DRX} = crystallographic density.

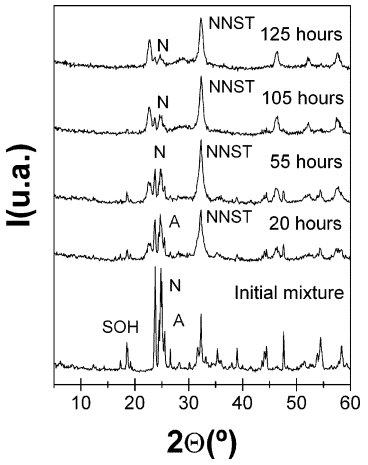

Figure 2. XRD patterns of the precursor corresponding to 0.9NaNbO$_3$−0.1SrTiO$_3$ ($x = 0.1$) composition after different milling times in a planetary mill (A = TiO$_2$ anatase, N = Nb$_2$O$_5$, NNST = $Na_{1-x}Sr_xNb_{1-x}Ti_xO_3$, SOH = Sr(OH)$_2$).

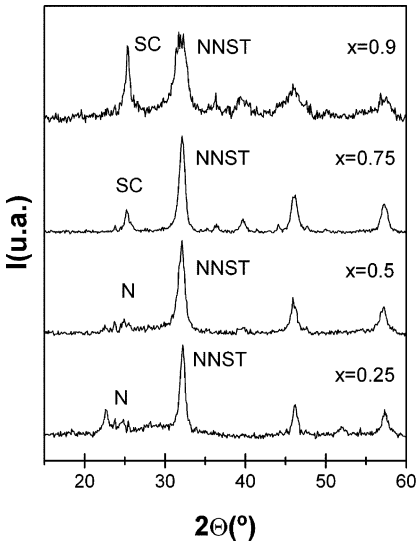

Figure 3. XRD patterns of the products obtained from the different precursors corresponding to $x = 0.25$, 0.5, 0.75, and 0.9 after 125 h of milling (N = Nb$_2$O$_5$, SC = SrCO$_3$, and NNST= $Na_{1-x}Sr_xNb_{1-x}Ti_xO_3$).

after 125 h of milling is formed mainly by the mechanosynthesized NNST perovskite, together with a small quantity of unreacted Nb$_2$O$_5$.

Similar results were obtained when the precursors corresponding to $x = 0.25$, 0.5, 0.75, and 0.9 were mechanochemically activated. In all cases, a perovskite NNST was the major phase, together with a small quantity of Nb$_2$O$_5$ in the case of $x = 0.25$ and 0.5 and of SrCO$_3$ for $x = 0.75$ and 0.9, as can be observed in Figure 3. In general, it can be said that higher Na−Nb contents imply shorter milling times for the mechanosynthesis of the perovskite.[22] This is in agreement with results by the conventional ceramic route.

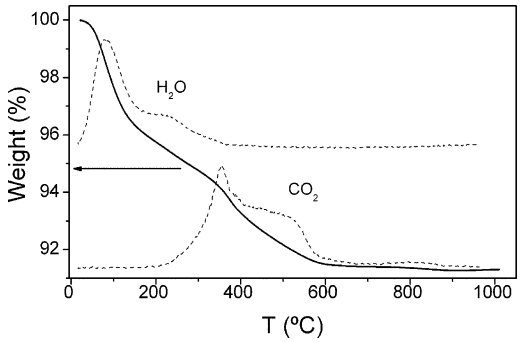

Figure 4. TG tracing and QMS measurements for masses corresponding to H$_2$O and CO$_2$, for the precursor corresponding to the composition 0.5(NaNbO$_3$)−0.5(SrTiO$_3$) mechanoactivated for 125 h.

In addition, the crystalline size obtained from XRD data by Scherrer's formula showed that the crystallite size of the perovskite mechanosynthesized decreases from 9 nm in the case of 0.9NaNbO$_3$−0.1SrTiO$_3$ to 6 nm in the case of 0.1NaNbO$_3$−0.9SrTiO$_3$. These facts point to the higher stability of the Na−Nb-rich phases, in good agreement with the diminution of the exothermic formation enthalpy with increasing Sr−Ti content that suggests a destabilization effect of the substation Na−Nb → Sr−Ti.[11]

The thermal behavior of the precursors activated for 125 h was investigated by TG, and the simultaneous mass spectrometry measurements gave information about the composition of the eliminated gases during the heating of the mechanoactivated samples. In Figure 4, the measurement corresponding to the composition of $x = 0.5$ (0.5NaNbO$_3$−0.5SrTiO$_3$) is shown as an example. Two important weight losses can be observed: one between room temperature and 300 °C, a step of 5% related to the elimination of H$_2$O, and the second one between 300 and 600 °C, of 3.5%, attributed to the carbonate decomposition and CO$_2$ elimination. This indicates that, during the milling, a small quantity of amorphous fraction was obtained together with the mechanosynthesized perovskite. This fraction contained hydroxides and carbonates formed in the activated sample by reaction with CO$_2$ and moisture from the atmosphere. The behavior of all the mechanoactivated samples is very similar, the main difference being the shift of the maximum of the CO$_2$ signal to higher temperatures when the quantity of the Sr−Ti increased. This is due to the mechanosynthesis of SrCO$_3$. This compound is more stable than the carbonates of sodium, and for this reason, the higher the Sr−Ti content, the higher the temperature of weight stabilization after the CO$_2$ elimination.

To isolate each perovskite as single phase, the mechanoactivated precursors were heated in a furnace at different

(22) Hungría, T. Ph.D. Thesis, Autónoma University of Madrid, 2005.

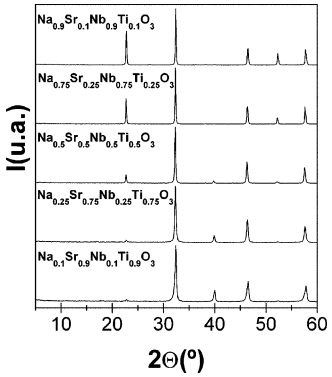

Figure 5. XRD patterns of the products obtained from the different precursors corresponding to $x = 0.1$, 0.25, 0.5, 0.75, and 0.9 after 125 h of milling and subsequent annealing at 800 °C for 12 h.

temperatures for 12 h. At temperatures higher than 600 °C, secondary phases completely disappeared, but the crystallinity of the perovskite was still low. Above this temperature, no other changes than those originating from crystalline growth were observed by XRD. Figure 5 depicts the XRD patterns of the different activated precursors annealed at 800 °C for 12 h. Peak splittings corresponding to the tetragonal and orthorhombic phases were not observed, probably due to their small particle size and subsequent peak broadening. In summary, the mechanosynthesis method allows the perovskite of the solid solution $(1-x)NaNbO_3-xSrTiO_3$ to be obtained at room temperature. Single phases are isolated after heating at temperatures as low as 600 °C, which represents a decrease of at least 600 °C in comparison with the solid-state route. This reduction has a twofold beneficial effect: to control particle growth and to avoid sodium volatilization and, thus, to improve stoichiometry control.

To investigate the nanosized nature of the samples obtained by mechanosynthesis, they were also investigated by TEM. An example of a characteristic TEM micrograph of the mechanosynthesized $Na_{0.25}Sr_{0.75}Nb_{0.25}Ti_{0.75}O_3$ perovskite is shown in Figure 6a. As can be observed, the sample is constituted by well-defined nanosized-crystalline particles. Analysis of the selected area electron diffraction, inset in the same figure, revealed that the majority of particles are crystalline and that the rings observed correspond to lattice spacings of 0.36, 0.29, 0.24, 0.20, 0.17, and 0.14 nm. These *d* values are consistent with both cubic ((100), (110), (111), (200), (211), and (220), respectively) and tetragonal perovskite-type structure ((002)−(200), (202)−(220), (222), (004)−(400), (204)−(402)−(420), and (404)−(440), respectively). This result corroborates the mechanosynthesis observed by XRD. The small size of these crystallites causes peak broadening in the XRD patterns, and rings to appear in the SAED pattern, so that the perovskite-type structures with different symmetries are indistinguishable in these nanometric mechanosynthesized samples. Figure 6b shows the particle size distribution of this nanosized sample obtained by Feret's diameter, from an ensemble of more than 100 crystalline particles. The particle size distribution is narrow: 95% of the studied particles have a diameter smaller than 15 nm. The average diameter is 9.1 nm, slightly higher than the value obtained from XRD data (8 nm). This difference is probably due to the broadening of the XRD peaks caused by internal stress not evaluated in Scherrer's formula.

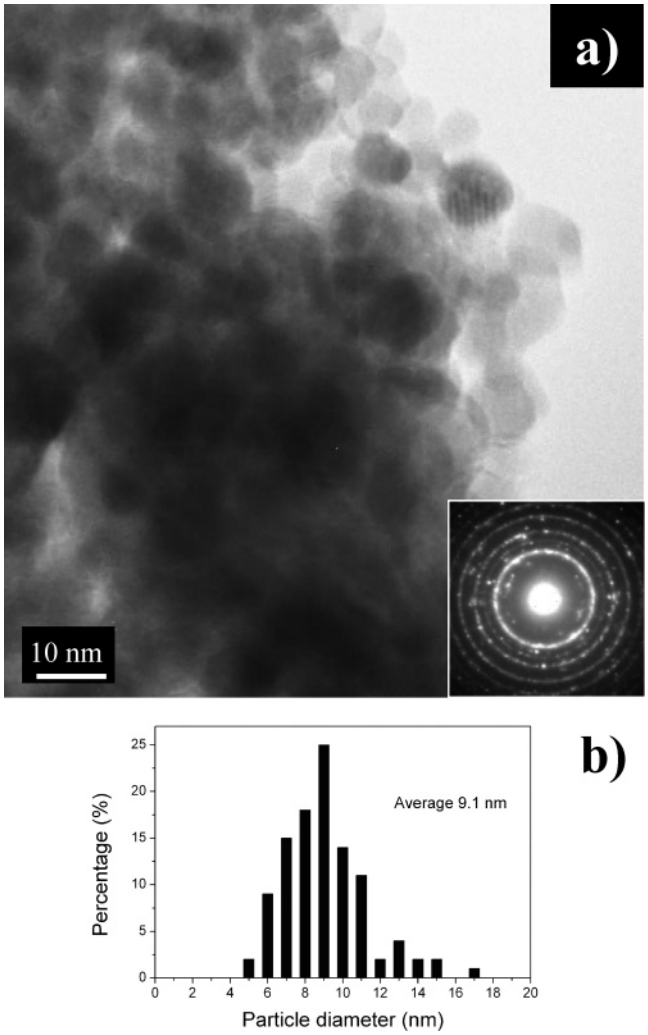

Figure 6. (a) TEM micrograph of the $Na_{0.25}Sr_{0.75}Nb_{0.25}Ti_{0.75}O_3$ mechanosynthesized powder. Inset: SAED of the zone. (b) Particle size distribution from TEM images of the mechanosynthesized sample.

Table 3. Processing Conditions for the $Na_{1-x}Sr_xNb_{1-x}Ti_xO_3$ Ceramics by Conventional Sintering at Different Temperatures for 2 h and Densities Obtained by the Archimedes' Method

composition	T (°C)	ρ (g cm^{-3})	$\rho_{relative}$ (%)
$Na_{0.9}Sr_{0.1}Nb_{0.9}Ti_{0.1}O_3$	1100	4.180	90.3
	1200	4.435	95.8
$Na_{0.75}Sr_{0.25}Nb_{0.75}Ti_{0.25}O_3$	1200	4.525	97.1
$Na_{0.5}Sr_{0.5}Nb_{0.5}Ti_{0.5}O_3$	1200	4.468	93.8
$Na_{0.25}Sr_{0.75}Nb_{0.25}Ti_{0.75}O_3$	1200	4.447	90.1
	1250	4.523	91.6
$Na_{0.1}Sr_{0.9}Nb_{0.1}Ti_{0.9}O_3$	1200	3.936	78.0
	1300	4.219	83.6
	1350	broken	

Ceramic Processing. $Na_{1-x}Sr_xNb_{1-x}Ti_xO_3$ ceramics were processed by conventional sintering from mechanosynthesized powders. XRD patterns of the ceramics prepared between 1200 and 1300 °C show that all of them are single phase. As is observed in Table 3, higher Sr−Ti contents resulted in lower density values at the same sintering conditions, except for the sample with $x = 0.1$. The high reactivity of the mechanosynthesized precursors allowed fully dense and crystalline ceramics to be obtained at 1200 °C in a single

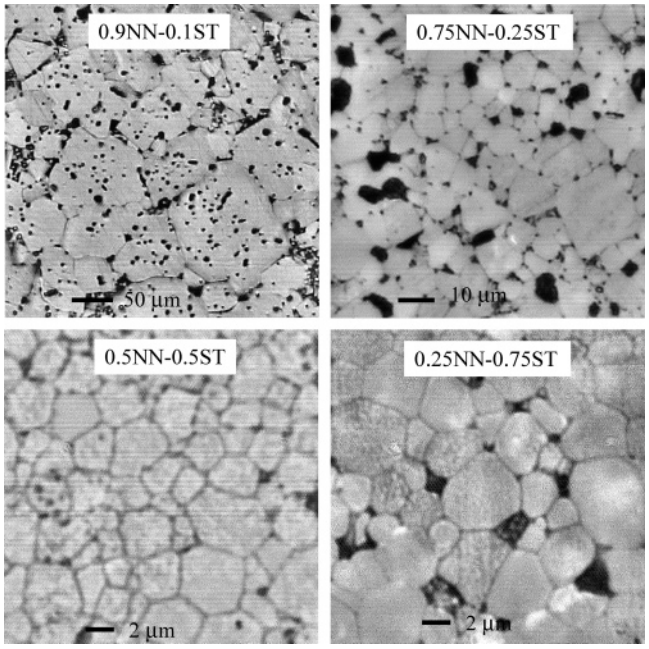

Figure 7. Microstructure of the $Na_{1-x}Sr_xNb_{1-x}Ti_xO_3$ ($1-x$NN$-x$ST) ceramics processed from the mechanosynthesized powder and sintered at 1200 °C for 2 h.

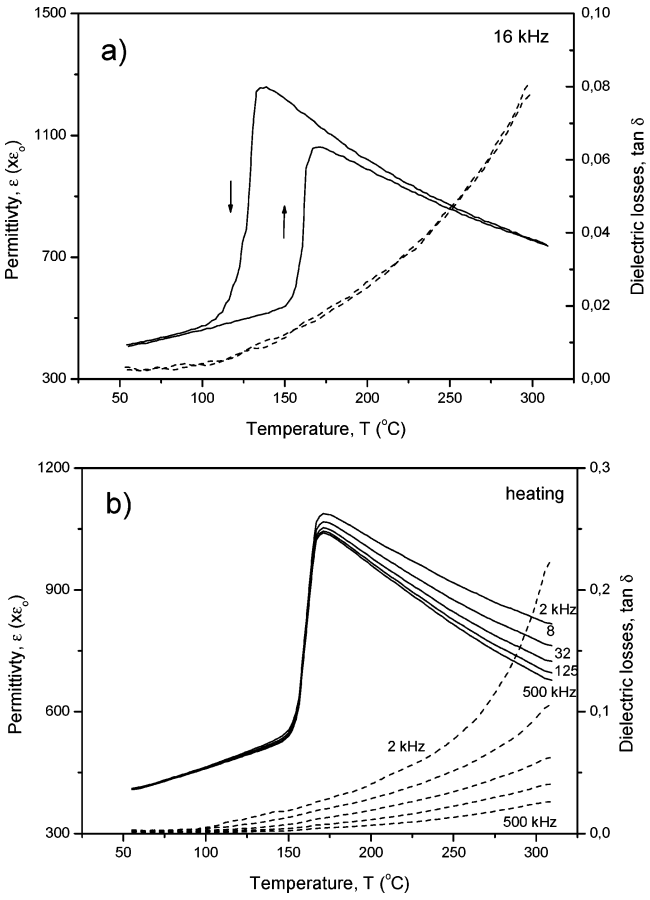

Figure 8. Temperature dependence of the dielectric permittivity and losses for a $Na_{0.9}Sr_{0.1}Nb_{0.9}Ti_{0.1}O_3$ ceramic processed from the mechanosynthesized powder and sintered at 1200 °C for 2 h: (a) at 16 kHz along a heating/cooling cycle and (b) on heating at five frequencies between 2 and 500 kHz.

thermal step. In the case of $Na_{0.1}Sr_{0.9}Nb_{0.1}Ti_{0.9}O_3$, the density of the ceramics was relatively low, even at 1300 °C, and the mechanical stability of the sintered sample was poor.

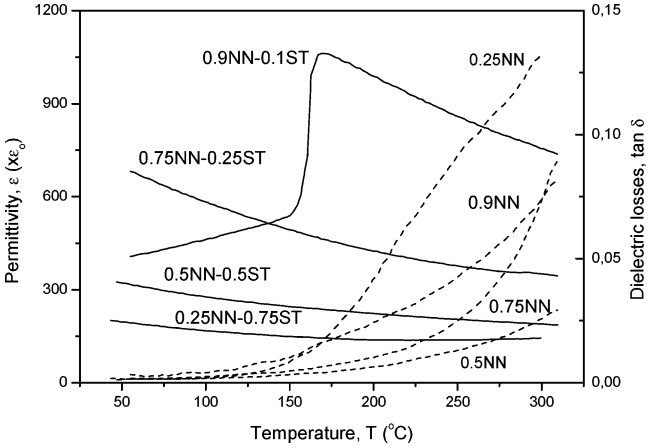

Figure 9. Temperature dependence of the dielectric permittivity and losses for $Na_{1-x}Sr_xNb_{1-x}Ti_xO_3$ ($1-x$NN$-x$ST) ceramics processed from the mechanosynthesized powder and sintered at 1200 °C for 2 h.

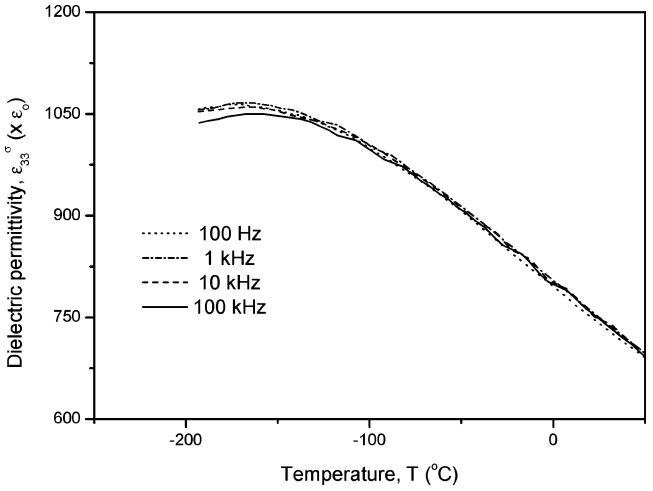

Figure 10. Temperature dependence below room temperature of the permittivity for the $Na_{0.75}Sr_{0.25}Nb_{0.75}Ti_{0.25}O_3$ ceramic.

Optical images of polished and thermally etched/quenched surfaces for the ceramic samples with $x = 0.1$, 0.25, 0.5, and 0.75 are shown in Figure 7. Abnormal grain growth has occurred for the ceramic with $x = 0.1$, for which very large, 50−100 μm, square-shaped grains are observed, which explains its lower density. This phenomenon is still present in the ceramic with $x = 0.25$, yet less significant, and it is absent from those with $x = 0.5$ and 0.75, for which a grain size of ∼3−5 μm is observed.

Electrical Characterization. Results on the temperature dependence of the dielectric permittivity for a $Na_{0.9}Sr_{0.1}Nb_{0.9}Ti_{0.1}O_3$ ceramic processed at 1200 °C from the mechanosynthesized powder are summarized in Figure 8. Permittivity at 16 kHz along a heating/cooling cycle is shown. A well-defined dielectric anomaly with a thermal hysteresis of ∼30 °C is observed. This anomaly resembles that associated with the first-order phase transition between the antiferroelectric, orthorhombic *Pbma* and *Pmmn* phases of $NaNbO_3$,[7] which is thus shifted from 360 to ∼150 °C by the addition of $SrTiO_3$ ($x = 0.1$). Permittivity measured on heating is shown in Figure 8b at five frequencies between 2 and 500 kHz. Hardly any dispersion is observed in the *Pbma* phase, while dc conduction is evident for the high-temperature *Pmmn* phase. The temperature dependence of the dielectric permittivity

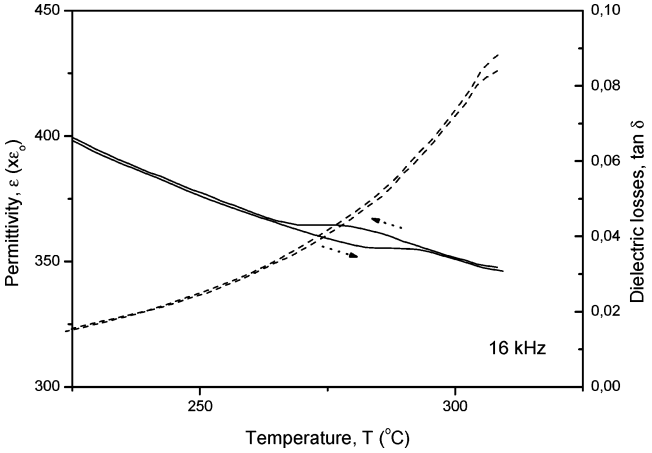

Figure 11. Detail of the temperature dependence of the permittivity and losses between 225 and 325 °C for the $Na_{0.75}Sr_{0.25}Nb_{0.75}Ti_{0.25}O_3$ ceramic.

for ceramics with increasing amount of $SrTiO_3$ is shown in Figure 9. Data at 16 kHz measured on heating from room temperature are presented. The dielectric anomaly associated with the *Pbma*−*Pmmn* phase transition is not observed for $x > 0.1$, which is in agreement with the room-temperature structural characterization by XRD that established the phase to be *Pmmn*. The occurrence of the transition for $Na_{0.75}Sr_{0.25}Nb_{0.75}Ti_{0.25}O_3$ below room temperature was investigated down to 77 K. These results are shown in Figure 10. No first-order phase transition-like anomaly was observed. Instead, a broad, slightly dispersive maximum appeared at ca. −165 °C, which suggests the existence of a low-temperature relaxor state that originates from the *Pmmn* phase. Above room temperature, the dielectric permittivity for the sample with $x = 0.25$ shows a tiny, yet distinctive, anomaly at 280 °C with a clear hysteresis as shown in Figure 11. This is most probably related to a first-order phase transition between the orthorhombic *Pmmn* phase and the tetragonal *I*4/*mmm* phase, the room-temperature phase for $x = 0.75$ according to the structural characterization.

Conclusions

Members of the solid solution $(1-x)NaNbO_3-xSrTiO_3$ in the whole range of compositions have been isolated as single phases by both the ceramic method and a mechanochemical activation route.

The structural characterization of the $Na_{1-x}Sr_xNb_{1-x}Ti_xO_3$ ($x = 0.1$, 0.25, 0.5, 0.75, and 0.9) solid solution showed that, with increasing Sr−Ti content, the symmetry of the oxides became higher, from orthorhombic for $x = 0.1$, 0.25, and 0.5 to tetragonal in the case of $x = 0.75$ and finally cubic for $x = 0.9$.

The combination of a wet-chemistry step and a mechanochemical process in a steel planetary mill led to the mechanosynthesis of nanosized particles of all the members of the $Na_{1-x}Sr_xNb_{1-x}Ti_xO_3$ solid solution at room temperature.

Single-phase, dense crystalline ceramics were obtained at 1200 °C in a single thermal step from the mechanosynthesized nanopowders with $x = 0.1$, 0.25, 0.5, and 0.75.

The sample with $x = 0.1$ is orthorhombic *Pbma* at room temperature and presents a first-order phase transition to the *Pmmn* phase at ∼150 °C with a thermal hysteresis of 30 °C. $x = 0.25$ is orthorhombic *Pmmn* at room temperature. This phase does not transform into the *Pbma* phase below room temperature, but a relaxor state evolves. Above room temperature, a first-order phase transition to the tetragonal *I*4/*mmm* occurs at 280 °C for this composition

Acknowledgment. The authors are thankful for financial support given by the Spanish MEC (MAT2004-00868 and MAT2005-01304) project. Teresa Hungría is indebted to the EU for the MIND network of excellence NMP3-CT2005-515757. The collaboration of Dr. E. Vila in the determination of the density of the isolated phases is greatly acknowledged. Thanks are also given to Dr. A. Landa for help with the transmission electron microscopy study of the samples, to Ms. I. Martinez and V. Martin for help with the ceramic samples preparation, and to Mr. Ph. Salles (CEMES, CNRS) in the electrical characterization below room temperature.

CM0614618